DIELECTRIC CONSTANT OF VEGETATION AT 8.5 GHz

N. L. Carlson

The Ohio State University

ElectroScience Laboratory

(formerly Antenna Laboratory)
Department of Electrical Engineering
Columbus, Ohio 43212

TECHNICAL REPORT 1903-5
31 March 1967

Contract NSR-36-008-027

National Aeronautics and Space Administration
Office of Grants and Research Contracts
Washington, D. C. 20546

NOTICES

When Government drawings, specifications, or other data are used for any purpose other than in connection with a definitely related Government procurement operation, the United States Government thereby incurs no responsibility nor any obligation whatsoever, and the fact that the Government may have formulated, furnished, or in any way supplied the said drawings, specifications, or other data, is not to be regarded by implication or otherwise as in any manner licensing the holder or any other person or corporation, or conveying any rights or permission to manufacture, use, or sell any patented invention that may in any way be related thereto.

The Government has the right to reproduce, use, and distribute this report for governmental purposes in accordance with the contract under which the report was produced. To protect the proprietary interests of the contractor and to avoid jeopardy of its obligations to the Government, the report may not be released for non-governmental use such as might constitute general publication without the express prior consent of The Ohio State University Research Foundation.

REPORT 1903-5

REPORT

by

The Ohio State University ElectroScience Laboratory
(Formerly the Antenna Laboratory)
Columbus, Ohio 43212

Sponsor	National Aeronautics and Space Administration Office of Grants and Research Contracts Washington, D. C. 20546
Contract Number	NSR-36-008-027
Investigation of	Radar and Microwave Radiometric Techniques for Geoscience Experiments
Subject of Report	Dielectric Constant of Vegetation at 8.5 GHz
Submitted by	N. L. Carlson ElectroScience Laboratory Department of Electrical Engineering
Date	31 March 1967

ABSTRACT

A cavity perturbation technique has been developed to measure the complex dielectric constant of vegetation at microwave frequencies. Several types of vegetation (grass, corn, spruce and taxus) were measured and the results showed that the dielectric constant of each is roughly proportional to the moisture content. For freshly cut samples, of about 65% moisture content, the dielectric constant was approximately 25-j7. As the samples were allowed to dry out the dielectric constant diminished to about 1.5 for ϵ' and .001 for ϵ''.

TABLE OF CONTENTS

DIELECTRIC CONSTANT OF VEGETATION
at 8.5 GHz

I. INTRODUCTION

In the past, much work has been done on dielectric and magnetic properties of chemical compounds and solutions.[1] However, comparatively little is known about the dielectric properties for substances found freely on earth. These include all types of vegetation and the many different kinds of rocks and soils.

The primary interest of this paper is with the measurement, at microwave frequencies, of the complex dielectric constant of vegetation, particularly the leaves, or in the case of coniferous plants, the needles. Because these materials are quite irregular in shape, and because their dielectric constant may be expected to depend on their water content, a cavity perturbation method was used. This permits accurate measurement of the properties of materials with the very large dielectric constant and loss tangent characteristic of water, and has the advantage of allowing samples of different shapes to be measured with the same equipment.

II. MICROWAVE CAVITY PRINCIPLES

The specimens of vegetation were measured in a microwave resonant cavity made from a section of X-band (8.2 to 12.4 GHz.) waveguide. One end of the waveguide was closed by a shorting wall and the other end was connected to a microwave network by a wall containing a small circular opening or iris, Fig. 1.

The effect of the iris is usually ignored in the elementary theory of cavity operation, in which it is customary to assume that the cavity is lossless, and has no wall openings. Practically, this is unrealistic, since losses are present, and since there must be some coupling between the cavity and the microwave network in order to measure the effect of introducing the sample. Using an iris to separate the cavity from the waveguide has the effect of replacing the short circuit of the ideal cavity with a large lumped susceptance. This susceptance will alter the conditions under which the cavity resonates and, accordingly, it will affect the rest of the microwave circuit.

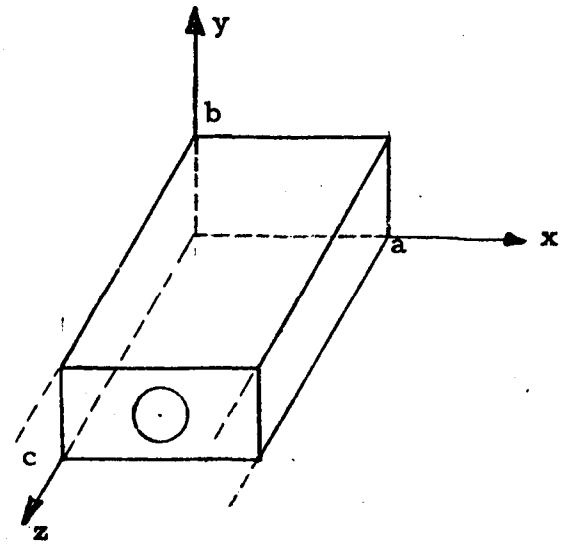

Fig. 1. The cavity with one end wall containing an iris.

The Idealized Cavity

In the absence of the iris and losses, the resonant frequency f_{res} is determined by the separation equation,

$$(1) \qquad \mu\epsilon\omega_{res}^2 = \left(\frac{m\pi}{a}\right)^2 + \left(\frac{n\pi}{b}\right)^2 + \left(\frac{p\pi}{c}\right)^2$$

$$(2) \qquad f_{res} = \frac{1}{2\sqrt{\mu\epsilon}}\sqrt{\left(\frac{m}{a}\right)^2 + \left(\frac{n}{b}\right)^2 + \left(\frac{p}{c}\right)^2}$$

where: a, b and c are the cavity dimensions; μ and ϵ are the permeability and permittivity of the medium filling the cavity.

This equation relates the resonant frequency of the cavity to its dimensions and to the permittivity and permeability of the material filling it. If the cavity dimensions are such that the dominant mode is the TE_{101}, the resonant frequency becomes,

$$(3) \qquad f_{res} = \frac{1}{2\sqrt{\mu\epsilon}}\sqrt{\frac{1}{a^2} + \frac{1}{c^2}}$$

The fields for the TE_{101} mode are:[2]

$$(4) \qquad E_y = E_o \operatorname{Sin}\left(\frac{\pi x}{a}\right) \operatorname{Sin}\left(\frac{\pi z}{c}\right)$$

$$(5) \qquad H_x = E_o\, ja \left(\frac{\mu}{\epsilon}\right)^{-\frac{1}{2}} (a^2 + c^2)^{-\frac{1}{2}} \operatorname{Sin}\left(\frac{\pi x}{a}\right) \operatorname{Cos}\left(\frac{\pi z}{c}\right)$$

$$(6) \qquad H_z = -E_o\, jc \left(\frac{\mu}{\epsilon}\right)^{-\frac{1}{2}} (a^2 + c^2)^{-\frac{1}{2}} \operatorname{Cos}\left(\frac{\pi x}{a}\right) \operatorname{Sin}\left(\frac{\pi z}{c}\right)$$

If losses are now considered, but still no iris is added, a quality factor or Q may be defined as follows:

$$(7) \qquad Q = \frac{\omega \times \text{energy stored}}{\text{average power dissipated}} = \frac{\omega \overline{W}}{\overline{P}_d}$$

The numerator and denominator of Eq. (7) may be determined from the usual expressions for stored energy [3]

$$(8) \qquad \overline{W}_m = \iiint \tfrac{1}{2} \mu |H|^2 \, dV$$

$$(9) \qquad \overline{W}_e = \iiint_{V \text{ cavity}} \tfrac{1}{2} \epsilon |E|^2 \, dv$$

Substituting Eq.(4) gives, for the electrical energy,

$$(10) \qquad \overline{W}_e = \frac{\epsilon}{2} \int_0^a \int_0^b \int_0^c E_o^2 \sin^2 \frac{\pi x}{a} \sin^2 \frac{\pi z}{c} \, dv$$

where: $\overline{W}_m$ = time average magnetic energy stored in cavity.
$\overline{W}_e$ = time average electric energy stored in cavity.
$\overline{P}_d$ = time average power dissipated within cavity.

Evaluating the integral yields the following result,

$$(11) \qquad \overline{W}_e = \overline{W}_m = \frac{\epsilon}{8} |E_o|^2 abc$$

The total amount of energy stored in the cavity at any time is just

$$2\overline{W}_m \text{ or } 2\overline{W}_e.$$

If it is assumed that all losses occur in the walls;[4]

$$(12) \qquad \bar{P}_d = R_m \iint |H|^2 \, d\bar{A}$$

where $R_m = \mathrm{Re} Z_m$, the real part of the surface impedance of the metal.[5]

$$(13) \qquad Z_m = \frac{1+j}{\sigma \delta_s} = R_m + jX_m$$

where $\delta_s = \sqrt{\frac{2}{\omega \mu \sigma}}$ and σ = the wall conductivity; the quantity δ_s is the skin depth of the metal. Substituting these relations into Eq. (7) yields the result for the TE_{101} mode.[6]

$$(14) \qquad Q = \frac{\pi \sqrt{\frac{\mu}{\epsilon}}\, b \left(a^2 + c^2\right)^{3/2}}{2 R_m \left[ac \left(a^2 + c^2\right) + 2b \left(a^3 + c^3\right)\right]}$$

Cavity Coupling

The effect of the iris -- that of placing a lumped susceptance in the waveguide -- may best be understood from the microwave circuit point of view. In the analysis which follows the iris is examined both as a lumped susceptance across a transmission line (waveguide) and as part of a lossless junction between two waveguides. By combining the two points of view, design criteria for the cavity are obtained. These criteria dictate both the resonant frequency and the effect of the cavity on the rest of the microwave network.

When the iris is looked upon as a lumped susceptance, Fig. 2, its position must be taken as coincident with the plane of symmetry of the actual iris in the waveguide. The impedance matrix for such an element has the following form.

$$(15) \qquad \left[\bar{Z}\right] = \frac{1}{jb} \begin{vmatrix} 1 & 1 \\ 1 & 1 \end{vmatrix}$$

The scattering matrix for this element may be determined from its impedance matrix by use of the relation,[7]

$$(16) \qquad \left[S\right] = \left[I\right] - 2\left[\bar{Z} + I\right]^{-1}$$

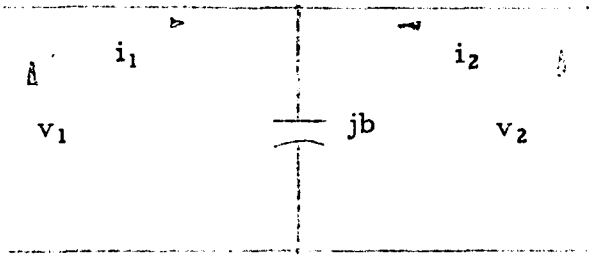

Note: jb is coincident with the plane of symmetry of the iris. The variables shown on the diagram are normalized as follows:

$$i = I\sqrt{Z_o} \; ; \quad v = V/\sqrt{Z_o} \; ; \quad jb = jB/Z_o$$

where V and I are the actual transmission line current and voltage and Z_o is the characteristic impedance.

Fig. 2. Diagram of a transmission line or waveguide with a lumped susceptance.

Substituting Eq. (15) and performing the required manipulation yields the desired [S] matrix,

$$[S] = \frac{1}{2j+b} \begin{vmatrix} -b & 2j \\ 2j & -b \end{vmatrix} \tag{17}$$

for an iris of susceptance b in a piece of waveguide, assuming that the reference planes are coincident with the plane of the iris.

The iris may also be viewed as a lossless junction, Fig. 3. The scattering matrix for any lossless junction has the general form:

$$(18) \qquad [S] = \begin{vmatrix} S_{11} & S_{12} \\ S_{21} & S_{22} \end{vmatrix} = \begin{vmatrix} -\sqrt{1-k^2} & jk \\ jk & -\sqrt{1-k^2} \end{vmatrix}$$

Physically the real quantity k is the coupling coefficient between the two transmission lines joined at the iris. In terms of the incident wave, a_1, and the transmitted wave, b_2, $k = b_2/a_1$ (see Fig 3).

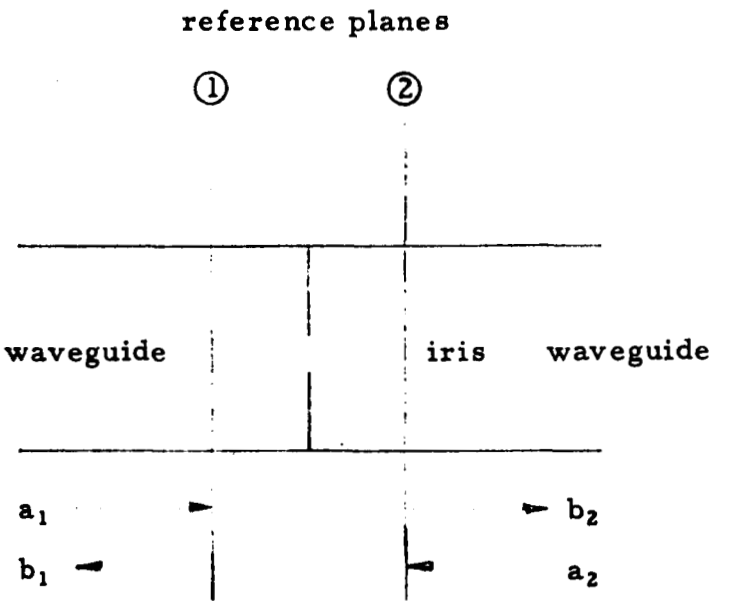

Fig. 3. A lossless junction formed by an iris in a waveguide; the corresponding reference planes are shown at ① and ②.

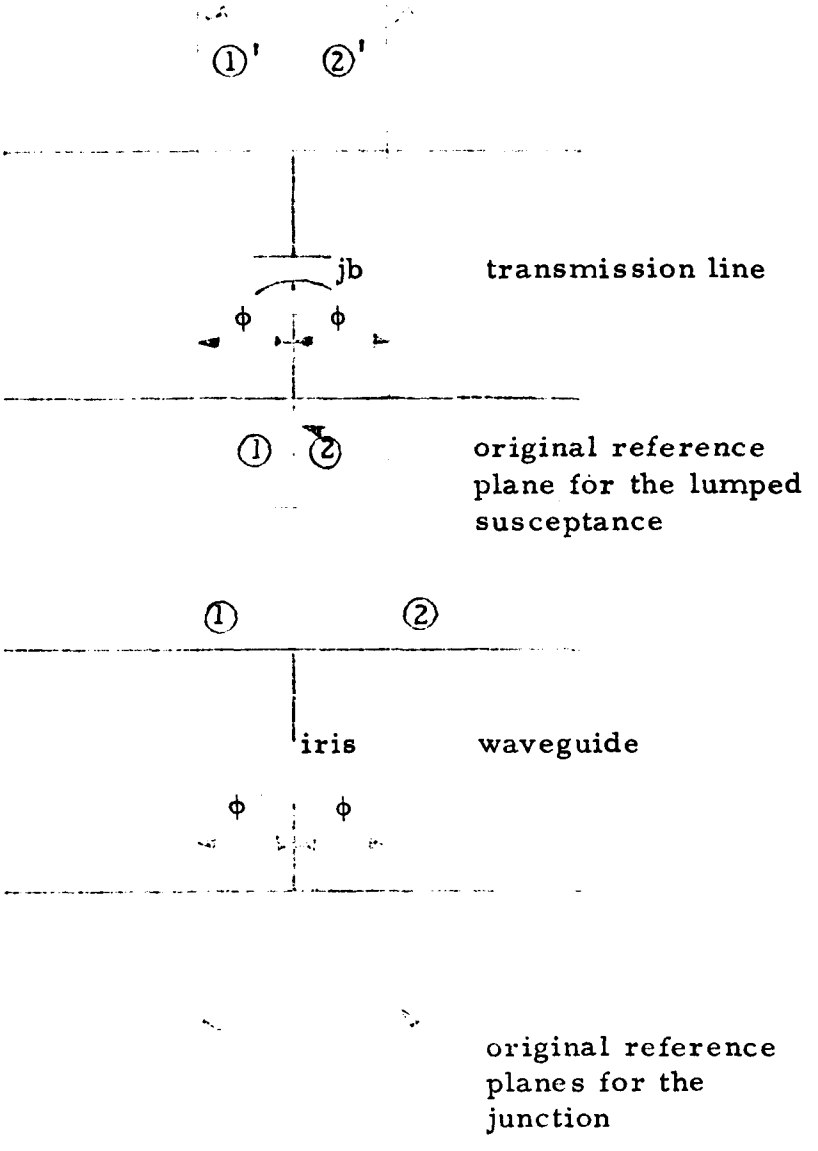

Fig. 4. The relation between the shift of reference planes for the lumped susceptance and the position of the reference planes of the iris.

Having determined the scattering matrices for a lumped susceptance on a transmission line and for a lossless junction in terms of its coupling coefficient, it is possible to relate the coupling coefficient to the susceptance. The problem at hand is to transform the scattering matrix for the lumped susceptance into the same form as that of the lossless junction and then compare the terms of the two matrices. This transformation is made by a change of reference plane position.

It may be seen[8] that the effect of shifting the reference planes of a junction outward is to create a new matrix, $[S']$ whose terms are related to those of the old matrix, $[S]$, as follows:

$$S'_{nm} = S_{nm} e^{j(\phi_n + \phi_m)} \tag{19}$$

where ϕ_n and ϕ_m are the electrical distances references planes n and m are shifted away from the junction. As an example, if reference planes 1 and 2 were shifted a distance ϕ_1 and ϕ_2 respectively, the new terms of the scattering matrix become:

$$S'_{11} = S_{11} e^{j(\phi_1 + \phi_1)}$$

$$S'_{12} = S_{12} e^{j(\phi_1 + \phi_2)}$$

$$S'_{21} = S_{21} e^{j(\phi_2 + \phi_1)}$$

$$S'_{22} = S_{22} e^{j(\phi_2 + \phi_2)}$$

If a reference plane is shifted toward the junction, it is considered to have been moved in the negative direction, while as in the example above, a move away from the junction is taken as positive. In the case of the lumped susceptance, Fig. 4, each reference plane is to be moved outward by the same distance, ϕ, so that the new scattering matrix is

$$[S'] = \frac{e^{j2\phi}}{2j+b} \begin{vmatrix} -b & 2j \\ 2j & -b \end{vmatrix} \tag{20}$$

This is the form taken by the S matrix of Eq. (17) when the reference planes have been moved a distance ϕ away from the junction.

By comparing S'_{11} and S'_{22} of Eq. (20) with S_{11} and S_{22} of Eq. (18) it may be seen that the terms of the two matrices will be of the same form, provided $\frac{-be^{j2\phi}}{2j+b}$ is real; that is,

$$(21) \qquad \phi = \frac{1}{2} \tan^{-1}\left(\frac{2}{b}\right).$$

The above transformation has been made for a capacitive iris, $+jb$. For an inductive iris, $-jb$, the reference planes must be moved in the negative direction, i. e. reference plane 1 must be moved across the junction to the side of port 2 and reference plane 2 must be moved to the side of port 1.

Once the matrix has been transformed, k may be determined by equating S'_{11}, S'_{22} in Eq. (20) with S_{11}, S_{22} in Eq. (18):

$$(22) \qquad k = \frac{\pm 2}{\sqrt{4+b^2}} \quad ,$$

the positive or negative sign being chosen as the iris is inductive or capacitive respectively.

If this junction (the iris) were now to be used as one end of a cavity, Fig. 5, the position of reference plane 2 becomes one of a voltage minimum, Fig. 6, i. e. it would represent the wall position in the ideal cavity. Since ϕ is known, the resonant frequency can thus be determined from the cavity dimensions and the susceptance of the iris. Since reference plane 2 takes the place of the missing solid wall, ψ (the electrical distance from the reference plane to the end wall) must be equal to $n\lambda_g/2$ (λ_g is the guide wavelength); for the TE_{101} mode this becomes just $\lambda_g/2$. The total cavity length at resonance in terms of the guide wavelength is:

$$(23) \qquad \ell = \frac{\lambda_g}{2} + \frac{\lambda_g \phi}{2\pi}$$

Substituting for ϕ

$$(24) \qquad \ell = \frac{\lambda_g}{2} + \frac{\lambda_g}{4\pi} \tan^{-1}\left(\frac{2}{b}\right)$$

$$(25) \qquad \frac{1}{\lambda_g} = \frac{1}{2\pi\ell}\left[\pi + \frac{1}{2}\tan^{-1}\left(\frac{2}{b}\right)\right]$$

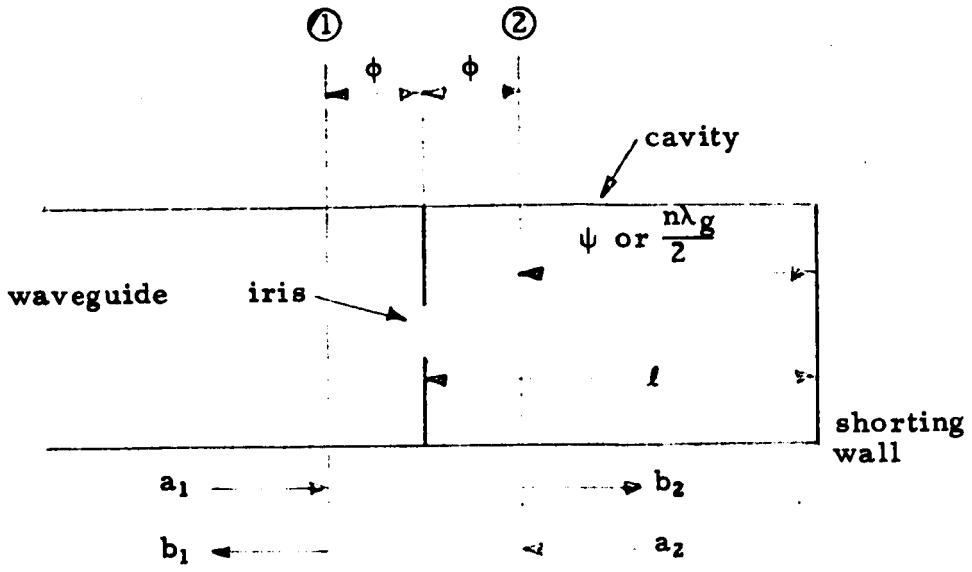

Fig. 5. One-port waveguide cavity.

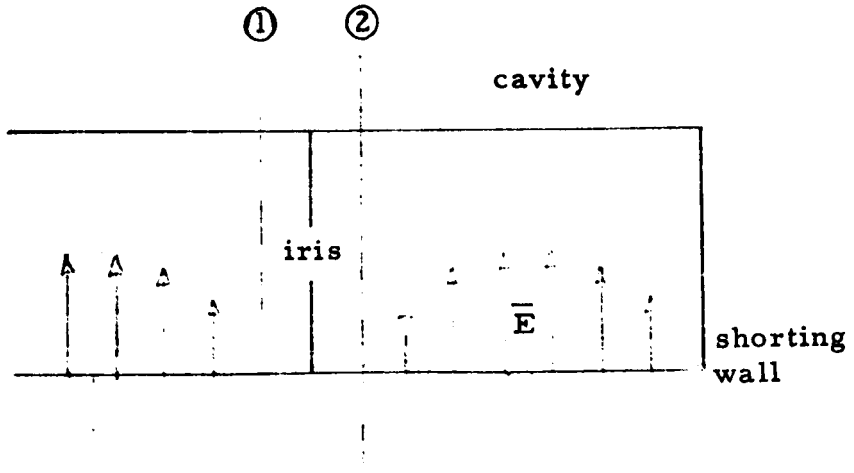

Fig. 6. The references planes become points of voltage minimums.

From the separation equation of the lossless waveguide,

$$(26)\quad -\left(\frac{2\pi}{\lambda_g}\right)^2 = \left(\frac{\pi}{a}\right)^2 - \left(2\pi f_{res}\right)^2 \mu\epsilon \ ,$$

so that

$$(27)\quad f_{res} = \frac{1}{2\sqrt{\mu\epsilon}} \sqrt{\left(\frac{1}{a}\right)^2 + \left(\frac{2}{\lambda_g}\right)^2} \ .$$

Substituting the relation for $\frac{1}{\lambda_g}$,

$$(28)\quad f_{res} = \frac{1}{2\sqrt{\mu\epsilon}} \sqrt{\left(\frac{1}{a}\right)^2 + \left[\frac{1}{\pi \ell}\left(\pi \pm \tan^{-1}\frac{2}{b}\right)\right]^2}$$

\+ for a capacitive iris

\- for an inductive iris

With this equation the cavity may be designed to resonate at any given frequency by varying ℓ, its length, and b, the iris susceptance.

Up until now the subject of losses and their effect on the choice of coupling coefficient has been avoided. Losses occur in the side and end walls of the cavity and in the iris itself. These losses may all be lumped together in a roundtrip attenuation constant such that a wave entering the cavity, traveling to the backwall and returning would be attenuated by the amount $e^{-\alpha_T}$; thus, (see Fig. 5).

$$(29)\quad a_2 = -b_2\, e^{-\left(\alpha_T + 2j\psi\right)}$$

Since the scattering parameters at the iris are related by the equation

$$(30)\quad \begin{vmatrix} b_1 \\ b_2 \end{vmatrix} = \begin{vmatrix} -\sqrt{1-k^2} & jk \\ jk & -\sqrt{1-k^2} \end{vmatrix} \begin{vmatrix} a_1 \\ a_2 \end{vmatrix}$$

one may substitute for a_2 to obtain:

(31) $$\frac{b_2}{a_1} = \frac{jk}{1-\sqrt{1-k^2}\ e^{-(\alpha_T+j2\psi)}}$$

(32) $$\frac{b_1}{a_1} = \frac{-\sqrt{1-k^2}+e^{-(\alpha_T+j2\psi)}}{1-\sqrt{1-k^2}\ e^{-(\alpha_T+j2\psi)}}$$

The first of these equations represents a transmission coefficient for the iris backed by a lossy cavity and the second gives the reflection coefficient. Differentiating b_2/a_1, with respect to k and then setting the result equal to zero allows the transmission coefficient, b_2/a_1, to be maximized.

(33) $$\frac{d\,b_2/a_1}{dk} = \frac{\sqrt{1-k^2}-e^{-(\alpha_T+j2\psi)}}{\left(1-\sqrt{1-k^2}\ e^{-(\alpha_T+j2\psi)}\right)^2\sqrt{1-k^2}} = 0$$

from this,

(34) $$\sqrt{1-k^2} = e^{-(\alpha_T+j2\psi)}$$

and since, at resonance, $\psi = \pi$ (for TE_{101}), there results the following relation between the attenuation and the coupling coefficient,

(35) $$\sqrt{1-k^2} = e^{-\alpha_T}$$

or

(36) $$k = \pm\sqrt{1-e^{-2\alpha_T}}$$

For this value of coupling, called the critical value, maximum power is transferred through the iris at resonance. At this critical value,

(37) $$\frac{b_2}{a_1} = \frac{\pm j}{\sqrt{1-e^{-2\alpha_T}}}$$

and

(38) $$\frac{b_1}{a_1} = 0$$

i.e. there is no reflected power, and the cavity is matched to the guide.

For values of $k \neq 1-e^{-2\alpha T}$ b_1 no longer equals zero at resonance. If $|k| < \sqrt{1-e^{-2\alpha T}}$, b_1, is negative and undercoupling results. In this case b_1 is affected more by reflection from the iris than backward flow from the cavity. When $|k| > \sqrt{1-e^{-2\alpha T}}$, the over-coupled case, the opposite is true and b_1 is dominated by backward flow from the cavity.[9]

With this analysis the cavity design criteria are complete. Using Eqs. (22, 28, and 36), a cavity with given losses may be designed to resonate at any given frequency, and its effect on the rest of the circuit may be determined.

The Quality Factor and the Microwave Circuit

With the addition of the iris to the cavity, defining a quality factor becomes more complicated. The previous definition, Eq. (7), was sufficient for the closed cavity since no interaction between the cavity and waveguide was present. With the introduction of the iris, three Q's must be defined. The first is the unloaded Q, Qu.

$$(39) \quad Qu = \frac{\text{Energy stored in the cavity}}{\text{Energy dissipated in the cavity per radian}}$$

This is the same Q as was defined earlier and it is independent of the effect of the coupling. The second is the external Q or Q_E,

$$(40) \quad Q_E = \frac{\text{Energy stored in the cavity}}{\text{Energy dissipated in the external circuit per radian}}$$

This definition must be qualified to mean the energy dissipated in the external circuit after the source has been shut off. (If this were not understood, and the cavity were critically coupled, b_1 would equal zero and Q_E would be infinite.) Last is the loaded Q or Q_L

$$(41) \quad Q_L = \frac{\text{Energy stored in the cavity}}{\text{Energy dissipated in both the cavity and external circuit per radian}}$$

Near its resonant frequency a microwave cavity may be thought of as a series R-L-C circuit, and the three Q's may then be determined from the element values by comparing the impedance expression for the cavity with that for the R-L-C circuit. The impedance in the cavity at a point immediately inside the iris and looking back into the cavity, Fig. 7, is given by the transmission line equation,

$$(42) \qquad Z = Z_o \frac{Z_r \cos\left(\alpha+j\beta\right)\ell + j\, Z_o \sin\left(\alpha+j\beta\right)\ell}{Z_o \cos\left(\alpha+j\beta\right)\ell + j\, Z_r \sin\left(\alpha+j\beta\right)\ell}$$

Z_r is the terminating impedance of the line, in this case zero. Eq. (42) thus reduces to:

$$(43) \qquad Z = Z_o \tanh\left(\alpha+j\beta\right)\ell = Z_o \frac{\tanh\alpha\ell + \tanh j\beta\ell}{1 + \tanh\alpha\ell \tanh j\beta\ell}$$

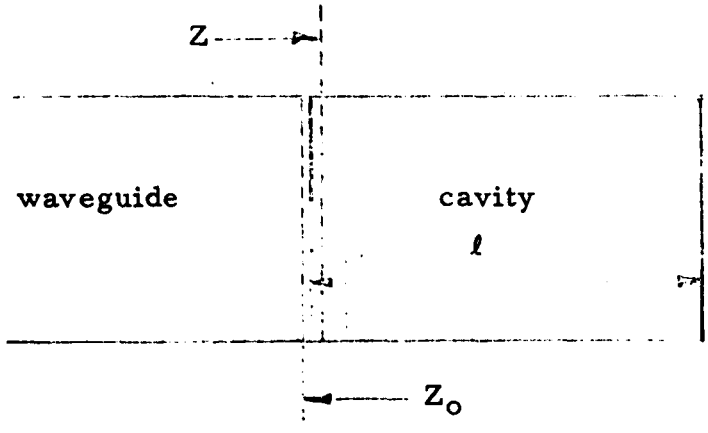

Fig. 7. The iris coupled cavity.

If the cavity losses are small,

$$\tanh\alpha\ell \approx \alpha\ell$$

and

$$(44) \qquad Z \approx Z_o \left(\alpha\ell + j\tan\beta\ell\right)$$

Also, for the TE_{101} mode, $\ell \approx \frac{\lambda_g}{2}$ at resonance so that

$$\tan\beta\ell \approx 0, \quad \alpha\ell\tan\beta\ell \ll 1$$

and,

$$(45) \qquad Z \approx Z_o \left(\alpha \ell + j\tan\beta \ell\right)$$

For small $\beta \ell$ this may be written in the form:[10]

$$(46) \qquad Z \approx Z_o \left(\alpha \ell + j \frac{\lambda g^2}{\lambda^2} \frac{\pi}{\omega_{res}} \delta\right)$$
$$\delta = \omega - \omega_{res}$$

This equation has the same form as the equation for the input impedance of a series R-L-C circuit:

$$(47) \qquad Z = R + j\left(\omega L - \frac{1}{\omega C}\right)$$

$$(48) \qquad Z \approx R + j2L\delta$$

where $\delta = \omega - \omega_{res}$

and $\omega^2_{res} = \frac{1}{LC}$

Matching the terms of Eqs. (46) and (48) gives,

$$(49) \qquad R = Z_o \alpha \ell$$

$$(50) \qquad L = \frac{Z_o}{2} \frac{\lambda g^2}{\lambda^2} \frac{\pi}{\omega_{res}}$$

The lumped susceptance of the iris and the characteristic impedance of the connected transmission line are in parallel with the R-L-C circuit. By combining the line impedance and the susceptance an equivalent series circuit may be drawn, Fig. 3. The parallel combination of $\frac{1}{jb}$ and Z_o is,

$$(51) \qquad \frac{Z_o/b^2 \; - \; j\, Z_o^2/b}{Z_o^2 \; + \; 1/b^2}$$

For a high Q circuit $Z_o^2 >> \frac{1}{b^2}$ so that the equivalent series combination becomes,

$$(52) \qquad \frac{1}{Z_o b^2} - j\frac{1}{b}$$

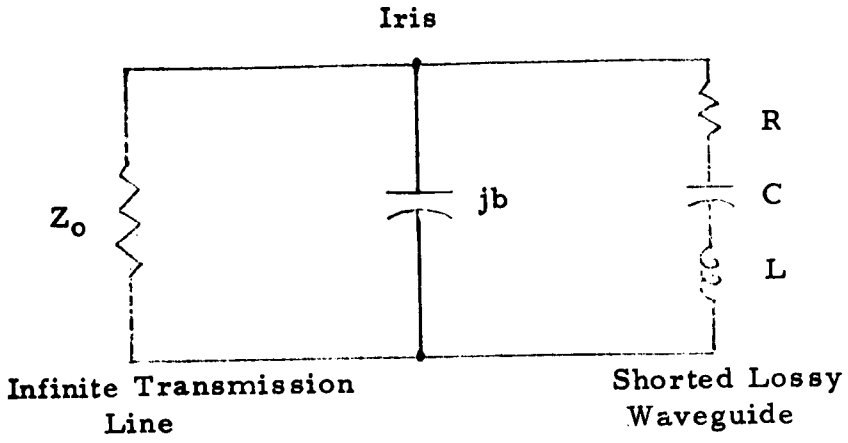

Fig. 8a. Equivalent circuit of an iris coupled cavity near resonance.

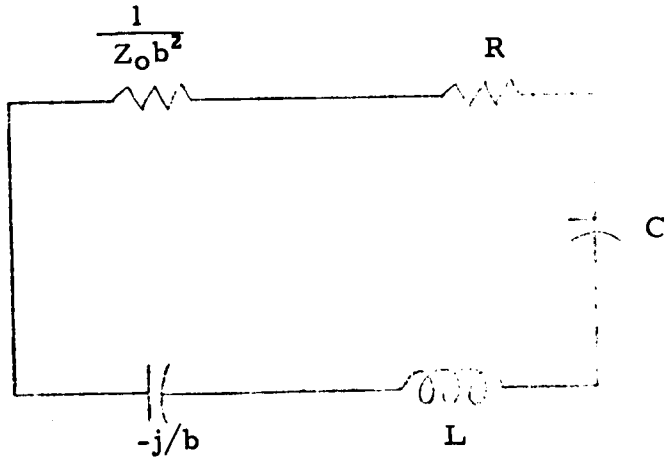

Fig. 8b. The equivalent series circuit.

From this circuit the unloaded Q is,

$$(53) \qquad Q_u = \frac{\omega_{res} L}{R}$$

$$(54) \qquad Q_u = \frac{\pi \lambda_g^2}{2\alpha \ell \lambda^2}$$

The external Q,

$$(55) \qquad Q_E = \left(\omega_{res} L - {}^{1}/_{b}\right) Z_o b^2$$

$$(56) \qquad Q_E = Z_o b \left(\frac{Z_o b \pi}{2} \frac{\lambda_g^2}{\lambda^2} - 1\right)$$

The loaded Q,

$$(57) \qquad Q_L = \frac{-{}^{1}/_{b} + \omega_{res} L}{{}^{1}/_{b^2} Z_o + R}$$

$$(58) \qquad Q_L = \frac{-b Z_o + b^2 Z_o^2 \frac{\pi}{2} \frac{\lambda_g^2}{\lambda^2}}{1 + b^2 Z_o^2 \alpha \ell}$$

III. PERTURBATION THEORY

If it were always possible to completely fill the cavity with a material, finding the dielectric constant of the material would be a relatively simple task. However, in many cases this is not practical, either because of a lack of homogeneity or because there is not enough sample material available. Under these circumstances, if the geometry of the sample is known, a perturbation method can be used to determine the dielectric constant. Here the electric field structure within the cavity is perturbed by the insertion of the dielectric sample, and by knowing the shape of the sample, its position in the cavity, and the change it produces in the resonant frequency and half power bandwidth of the cavity, the complex dielectric constant of the sample may be determined. If the sample has a relative permeability of unity, its position in the cavity is not important since the magnetic field will not be disturbed. On the other hand, if the relative permeability is not unity, care must be taken to put the sample where the magnetic field is zero or almost zero. With the TE_{101} mode, this corresponds to a line passing through the center of the cavity parallel to the y axis, Fig. 1a. It is also possible to measure the permeability of a sample with this method by placing the sample at a position of zero electric field.

To determine quantitatively the effect of perturbing the cavity, consider first the situation of Fig. 9a. which represents the cavity in the unperturbed case. $\bar{E}_o$, $\bar{H}_o$ represent the unperturbed fields and ϵ and μ represent the homogeneous medium enclosed by the cavity. Fig. 9b. shows the perturbed case with the new fields $\bar{E}$, $\bar{H}$ and a new dielectric constant, $\epsilon+\Delta\epsilon$. Having defined these fields, an expression may be arrived at which relates the change in the resonant frequency to the addition of a sample with a dielectric constant $\epsilon+\Delta\epsilon$[11].

$$(59) \qquad \frac{\omega - \omega_o}{\omega} = - \frac{\iiint \left(\Delta\epsilon \, \bar{E}\cdot\bar{E}_o^*\right) dv}{\iiint \left(\epsilon \, \bar{E}\cdot\bar{E}_o^* + \mu \bar{H}\cdot\bar{H}_o^*\right) dv}$$

where ω and ω_o are the perturbed and unperturbed resonant frequencies, respectively. This equation is the exact relation for the change in resonant frequency if $\bar{H} = O$ at the point where the cavity is perturbed or if μ is always unity. Since the field inside the perturbed cavity is unknown, except for some very simple sample shapes, an approximation is needed to provide a simple expression for the electric field inside the perturbed cavity. The sample shape of interest here is a thin rectangular cylinder positioned such that its long direction is parallel to the electric field, Fig. 10. Applying the boundary conditions for a field tangential to the flat surface of the sample shows that the electric field immediately inside the sample must be the same as that outside. Furthermore, as long as the thickness (t) of the sample is much less than a skin depth, the field throughout the sample will be nearly equal to the external field, that is to the unperturbed electric field. The perturbed field in the rest of the cavity may also be approximated by the original field since the volume of the sample is small compared to the volume of the cavity. Substituting these approximations into Eq. (59) gives,

$$(60) \qquad \frac{\omega-\omega_o}{\omega} \approx - \frac{\iiint \Delta\epsilon \, E_o^2 \, dv}{\iiint \left(\epsilon \left| E_o \right|^2 + \mu \left| H_o \right|^2\right) dv}$$

Now since, $\epsilon \left|E_o\right|^2 = \mu \left|H_o\right|^2$ and, $\Delta\epsilon = \epsilon_o \left(\epsilon_r - 1\right)$

$$(61) \qquad \frac{\omega-\omega_o}{\omega} \approx - \frac{\left(\epsilon_r - 1\right)}{2} \frac{\iiint E_o^2 \, d\Delta v}{\iiint E_o^2 \, dv}$$

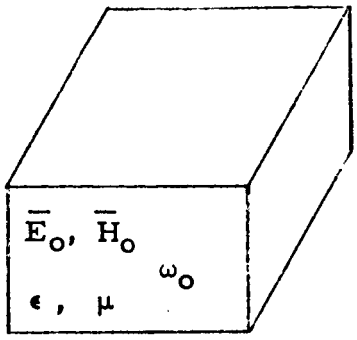

Fig. 9a. The cavity as originally unperturbed.

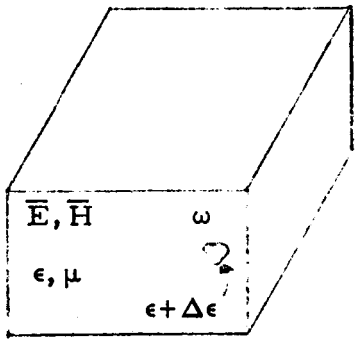

Fig. 9b. The cavity as perturbed by a small dielectric sample.

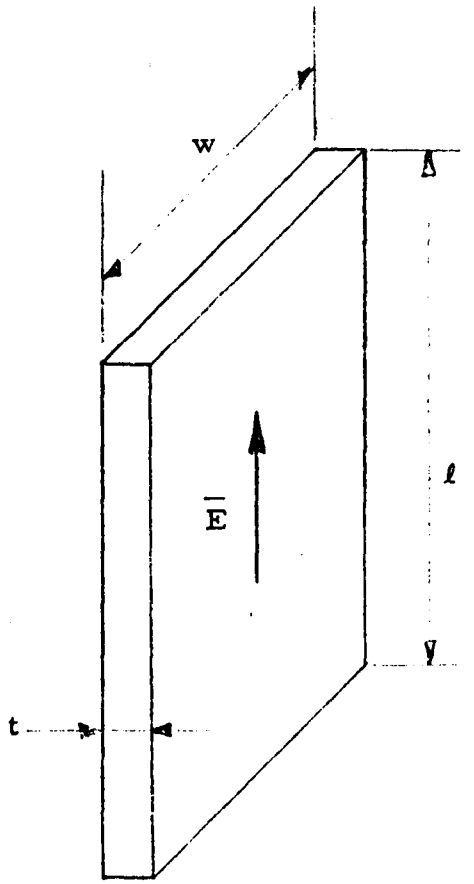

Fig. 10. The sample shape and its orientation with respect to the $\overline{E}$ field.

The numerator is integrated only over the volume of the sample, Δv, since $\Delta\epsilon = \epsilon_r - 1$ and is zero everywhere else in the cavity.

The sample is placed in the center of the cavity, Fig. 11 for several reasons; the electric field is greatest at this point and therefore a sample placed there would affect the cavity resonance more than if it had been placed elsewhere; there is the least amount of position error since the field remains almost constant over small distances from the center; the magnetic field is zero.

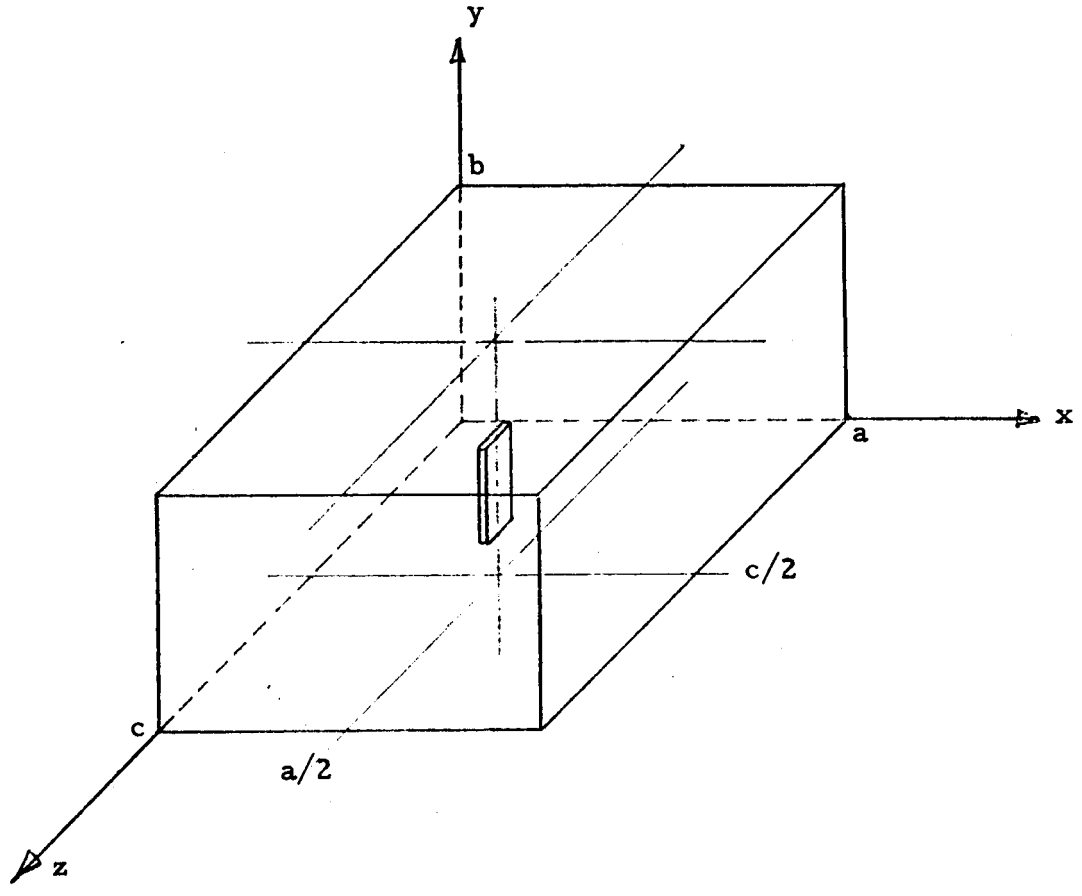

Fig. 11. The sample position in the cavity with t << a and w << c.

Evaluating Eq. (61) with the sample in the center and using the TE_{101} field expression yields:

$$\frac{\omega-\omega_o}{\omega} \approx -\frac{\epsilon_r-1}{2} \frac{\int_{\frac{b-\ell}{2}}^{\frac{b+\ell}{2}} \int_{\frac{a-t}{2}}^{\frac{a+t}{2}} \int_{\frac{c-w}{2}}^{\frac{c+w}{2}} \sin^2 \frac{\pi x}{a} \sin^2 \frac{\pi z}{c} \, dydxdz}{\int_o^b \int_o^a \int_o^c \sin^2 \frac{\pi x}{a} \sin^2 \frac{\pi z}{c} \, dydxdz} \tag{62}$$

This reduces to the following:

$$(63) \qquad \frac{\omega-\omega_o}{\omega} \approx - \frac{2(\epsilon_r-1)\ell tw}{a\,b\,c}$$

If the perturbing sample is lossy, $\epsilon_r = \epsilon' - j\epsilon''$, the resonant frequency is complex, and may be expressed in the form[12]

$\omega = \omega_{res} + j\frac{\omega_{res}}{2Q_u}$.

Substituting these in Eq. (63):

$$(64) \qquad \frac{\omega + j\frac{\omega_o}{2Q} - \omega_o - j\frac{\omega_o}{2Q_o}}{\omega + j\frac{\omega}{2Q}} \approx - 2\left(\epsilon'-1-j\epsilon''\right)\frac{\ell tw}{a\,b\,c}$$

where Q = the unloaded Q of the perturbed cavity

Q_o = the unloaded Q of the unperturbed cavity

In the denominator, $\frac{\omega}{2Q}$ may be assumed negligible compared to ω and the equation may be broken into real and imaginary components. For the real part,

$$(65) \qquad \frac{\omega-\omega_o}{\omega} \approx - 2\left(\epsilon'-1\right)\frac{\ell tw}{a\,b\,c}$$

and since $\omega \approx \omega_o$, the imaginary part becomes

$$(66) \qquad \frac{1}{Q} - \frac{1}{Q_o} \approx 4\epsilon'' \frac{\ell tw}{a\,b\,c}$$

Eqs. (65) and (66) relate the change in resonant frequency and the change in Q_u to the complex dielectric constant of a sample perturbing the cavity. Similar relationships could also be derived for a sample perturbing the magnetic field in order to determine the complex permeability. For samples of other shapes but which satisfy the condition that the internal electric field is approximately equal to the unperturbed electric field, one may still use equations 65 and 66, with the quantity (ℓtw) replaced by the volume of the sample. Suitable samples shapes are thin sheets of material with the "thickness" dimension perpendicular to the unperturbed electric field. Appropriate approximate fields for cylindrical and spherical samples are given in a previous reference.[11]

IV. THE MICROWAVE EQUIPMENT

This section describes the microwave network used to make the dielectric measurements and the principles behind its operation. The microwave circuit is shown in Fig. 12. All of the components except the cavity and iris are readily-available commercially-made items.

The operation of this network depends upon the properties of the magic tee. For the moment assume that the iris has been replaced by a shorting wall but that the rest of the equipment remains unchanged. Power from the klystron which enters port 3 is split equally between ports 1 and 2. The resultant waves travel down lines 1 and 2, and are reflected by the shorting plate of line 1 and the sliding short of line 2. Now, if the sliding short of line 2 is adjusted so that its distance from the junction is equal to that of the shorting wall of line 2, both the reflected waves of lines 1 and 2 arrive back at the junction in phase. Power from lines 1 and 2 is again split equally, this time between ports 3 and 4. No power is transmitted from port 1 to 2 or from 2 to 1. Because of the fact that the signals from lines 1 and 2 enter line 4 with opposite phase, the resultant signal in line 4 is zero. The power entering port 3 is absorbed by the isolator and attenuator, and is no longer of any consequence.

The same situation also occurs with the arrangement of Fig. 12, using the iris and cavity in line 1 instead of the shorting wall, as long as the frequency is well off resonance where the iris acts almost as a short circuit. As the frequency of the system approaches resonance, power will begin to be dissipated in the cavity. Since the power now absorbed within the cavity would otherwise have been reflected, the difference between the two waves entering port 4 is no longer zero and the power meter at the end of line 4 will indicate a change in power level. The power meter connected to line 4 measures, in fact, a portion of the power absorbed in the cavity, and by noting the frequencies for which the power level is 3 db below that at resonance, the half power bandwidth may be determined. (See Appendix A). The resonant condition of course, is determined by the frequency at which maximum power is absorbed.

In practice, determining the half power bandwidth by changing the frequency leads to difficulties which can be avoided by always operating at the same frequency, and changing the cavity dimension to provide a resonance effect. This is accomplished by replacing the end wall of the cavity with a calibrated sliding short, Fig. 13. The resonant frequency of the cavity may now be increased or decreased by moving this short in or out. A curve may be plotted to relate the short position and the resonant frequency; a typical example is given in Fig. 14.

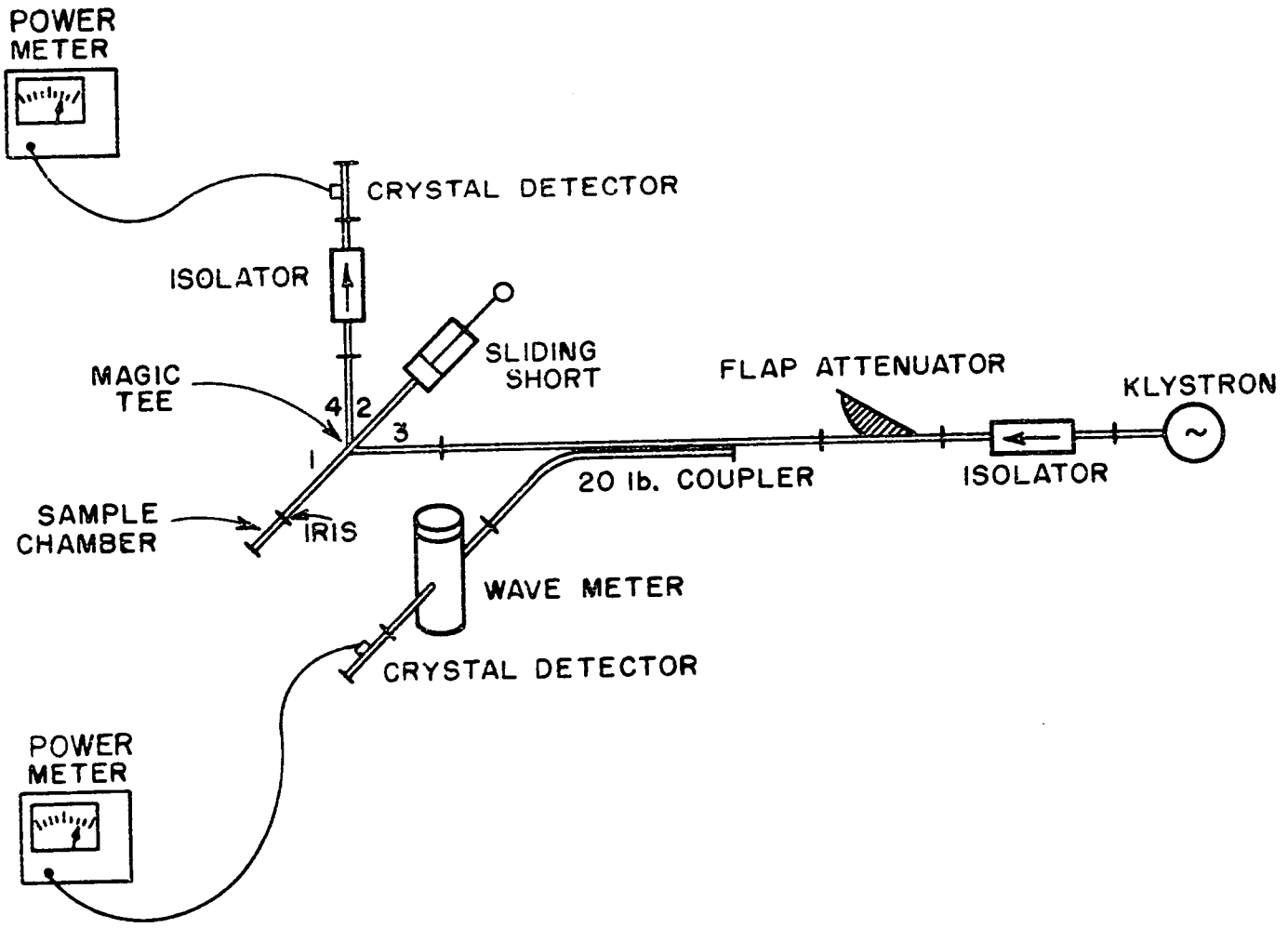

Fig. 12. Equipment for the measurement of the dielectric constant and loss tangent of vegetation.

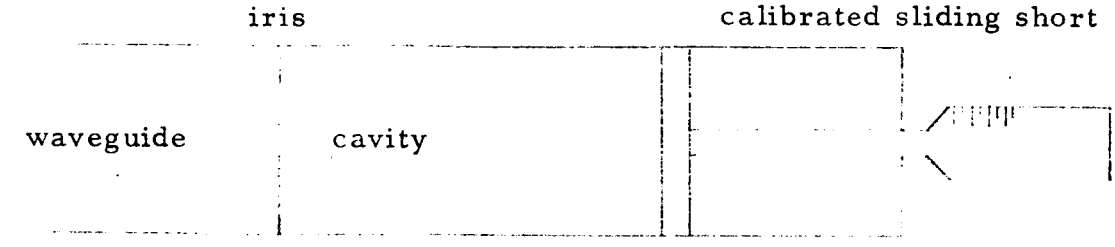

Fig. 13. The cavity with a calibrated sliding short replacing the solid end wall.

It will be noticed that the curve is linear over the small frequency range covered by Fig. 14, and frequency measurement can be made with very little error. This method has two advantages over changing the system frequency. Changing either the turning screw or reflector voltage of a klystron, besides altering its frequency, also changes the output power level. It is evident that this would make any attempt at determining the half power bandwidth, and thus ϵ'' futile. Furthermore, if the system frequency were varied and the path lengths of lines 1 and 2 were not equal, the sliding short of line 2 would have to be adjusted along with the frequency in order to keep the two waves entering port 4 exactly 180° out of phase.

V. MEASUREMENT PROCEDURE

Once one is familiar with the equipment and its operation, the measurement procedure is relatively simple. For the measurements reported here the sample was held in place at the center of the cavity by a styrofoam block. Thus the "unperturbed"cavity, (the condition under which the frequency calibration curve of Fig. 14 was plotted) contained the styrofoam. The "perturbed" cavity contained both the styrofoam and the sample. Once the cavity was in place (either perturbed or unperturbed), the sliding short on the cavity was moved to a position where the cavity would not be near resonance. Next the sliding short on line 2, Fig. 12, was adjusted to produce a null on the meter. Having done this, the sliding short on the cavity was moved

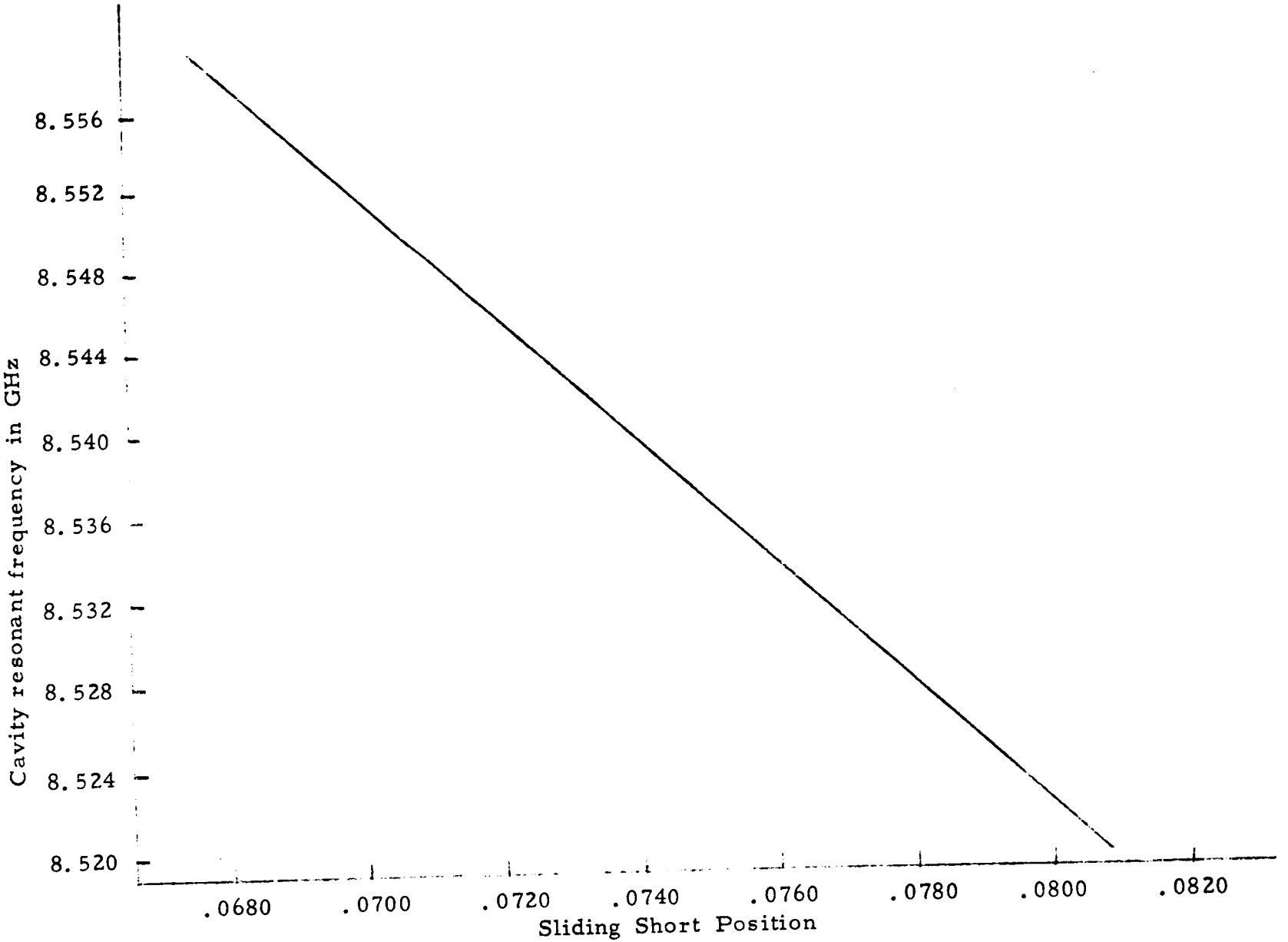

Fig. 14. Sliding short-cavity resonant frequency calibration curve.

through resonance, and the resonance and half power short positions were noted and converted to equivalent frequencies. When the cavity was perturbed the resonant frequency determined by the short position from the calibration curve, ω_o, was different from the actual operating frequency, ω. In this case perturbing the cavity lowered the resonant frequency, provided the dimensions were kept constant. Therefore, the short had to be moved inwards to make the cavity resonate again at the system frequency. Moving the cavity end wall inward resulted in a resonant short position which corresponds to a "frequency" higher than the system frequency.

For some high dielectric samples which produce a large change in frequency, ω_o may not be within the frequency calibration curve. In these instances either the curve must be extended, or more conveniently, the system frequency, ω, can be changed until ω_o and the half power frequencies again lie within the limits of the curve. If this is done, ω must be measured with a wave meter to find the change in frequency, $\omega-\omega_o$.

The operation of the system was checked by measuring the frequency shifts and bandwidth of a very thin glass tube filled with water, retained within the cavity by a styrofoam block, and with the axis of the tube parallel to the electric field. The roughly cylindrical sample was considered to be an ellipsoid of revolution having the same major and minor axis as the actual sample, and an internal field correction was computed from standard tables.* Fairly good agreement was obtained between the measured value of ϵ and the tabulated value for the same temperature and frequency, with the measured values consistently 10% to 15% low.

VI. CAVITY MEASUREMENT RESULTS

The motivation for the measurements taken here was to provide a basis for a theory of radar return from vegetation (in all models of which, the dielectric constant of plant material must be known) as well as interest in the dielectric constant of vegetation for its own sake. In order to provide a range of plant types to compare with available radar measurements,[13] four different kinds of plants were measured:

grass - small strips were cut from blades of common lawn grass.
corn - strips were cut from the broad leaves of the plant, just before tasseling.
taxus cuspidatus (yew) - small portions of the needles were used from this evergreen shrub.
blue spruce - small portions of the needles were used from this evergreen tree.

* B. Lax and K. J. Button, Microwave Ferrites and Ferri magnetics. New York 1964 p. 162.

With each of these samples the specimens were cut quite small, typically .005" x. 1" x. 05" and were placed in the cavity with their vein structure parallel to the electric field. The fact that the samples were so small made accurate measurement of the dimensions difficult and this proved to be the major source of error in the results. The skin depth for these samples was calculated and was found to be 0.16 inches. In view of the small sample size, the approximation that the electric field in the sample is the same as that outside is correct.

The dielectric constant measurements were made using the cavity perturbation technique discussed previously and the results of these measurements are displayed in Figs. 15 - 17. After a sample piece was freshly cut its physical dimensions were measured using an optical comparator. The electrical properties were then measured in the cavity and the weight was recorded immediately afterwards, using a Cahn Electrobalance. The same sample piece was then continuously measured and weighed until it had completely dried out. Each line on Figs. 15 - 17 indicates the progress of an individual sample piece as it was allowed to dry out. Final drying to determine the dry weight was carried out in a small oven.

The normal operating frequency of the system was 8.5 GHz, and the insertion of a sample in the cavity changed the resonant frequency by as much as 50 MHz. (which could be measured with a precision of approximately 1 MHz) for a freshly cut piece and as little as 1 MHz. for a dried out piece. Typically, Q_u, when the cavity was perturbed by a freshly cut specimen, was about 200. As the sample dried, Q_u usually increased to a high of about 1200; taxus cuspidatus was an exception with a Q_u of only 600 for a dried sample. The Q_u for the unperturbed cavity was 1400.

As the samples dried out, their dielectric constants changed. For this reason the dielectric constant was plotted as a function of the moisture content. The measured dielectric constants and the respective weights were then used to plot the curves of Figs. 15 - 18. Moisture content was determined from the weight as follows:

$$(67) \qquad \% \text{ moisture content} = \frac{(\text{sample wgt.} - \text{dry wgt.}) \times 100}{\text{sample wgt.}}$$

All of the samples were found to dry out extremely rapidly - so much so that some of the water was undoubtedly lost between measuring and weighing. For this reason, the plotted values of water content are probably systematically smaller than the actual values at the time of measurement. Although the precision of measurement was not adequate to reveal temperature effects, it may be noted that most of the data was taken at temperatures between 75° F. and 95° F.

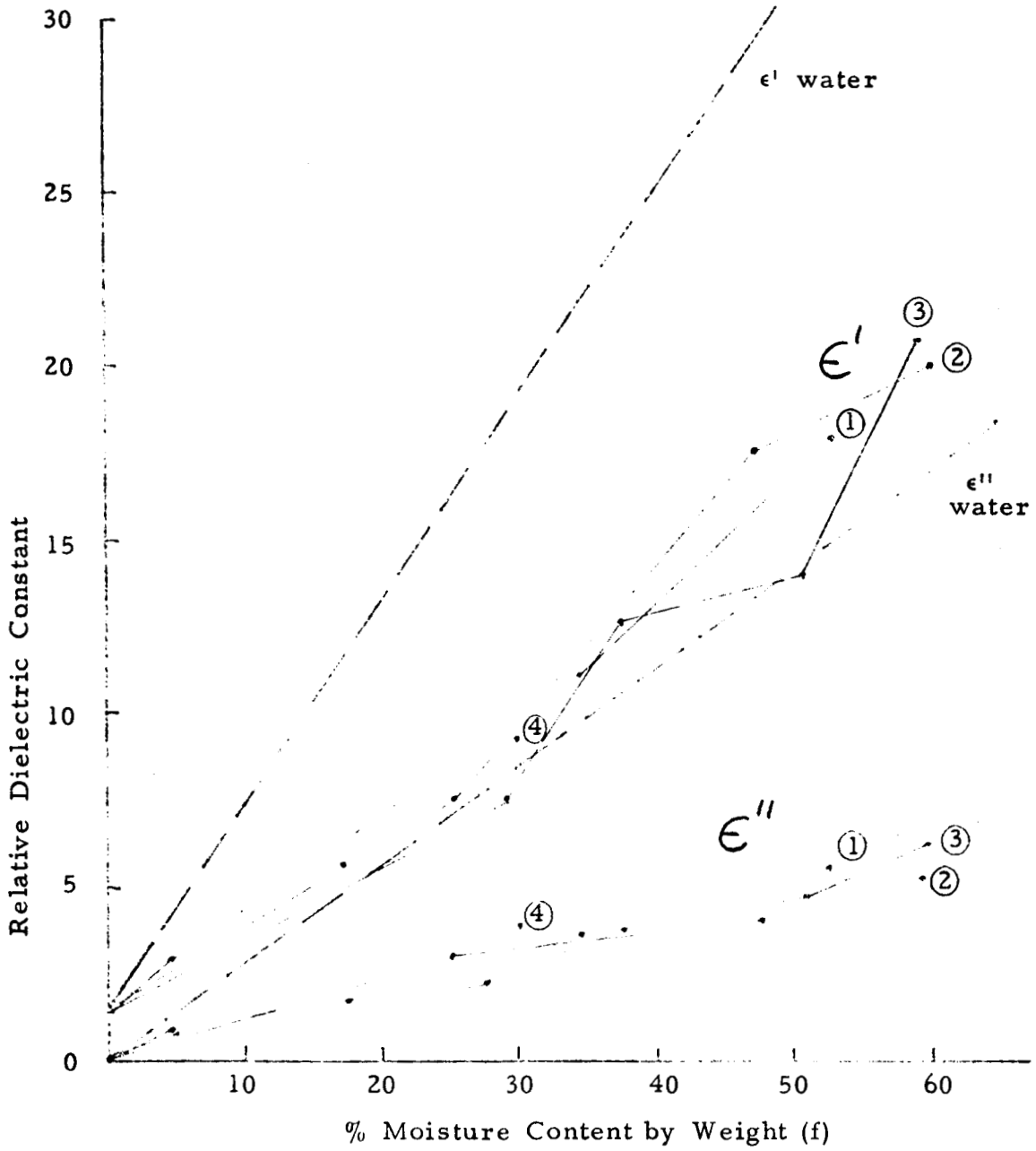

Fig. 15. The complex dielectric constant of grass leaf plotted as a function of moisture content. The numbers on the two curves, ϵ' and ϵ'', represent the same sample and the curves show the progress of the sample as it dried out. The dashed curve is the equation $1.5 + (\epsilon'_w - j\epsilon''_w) \times f$ where $\epsilon'_w - j\epsilon''_w$ is the dielectric constant of water and f is the fraction of water content.

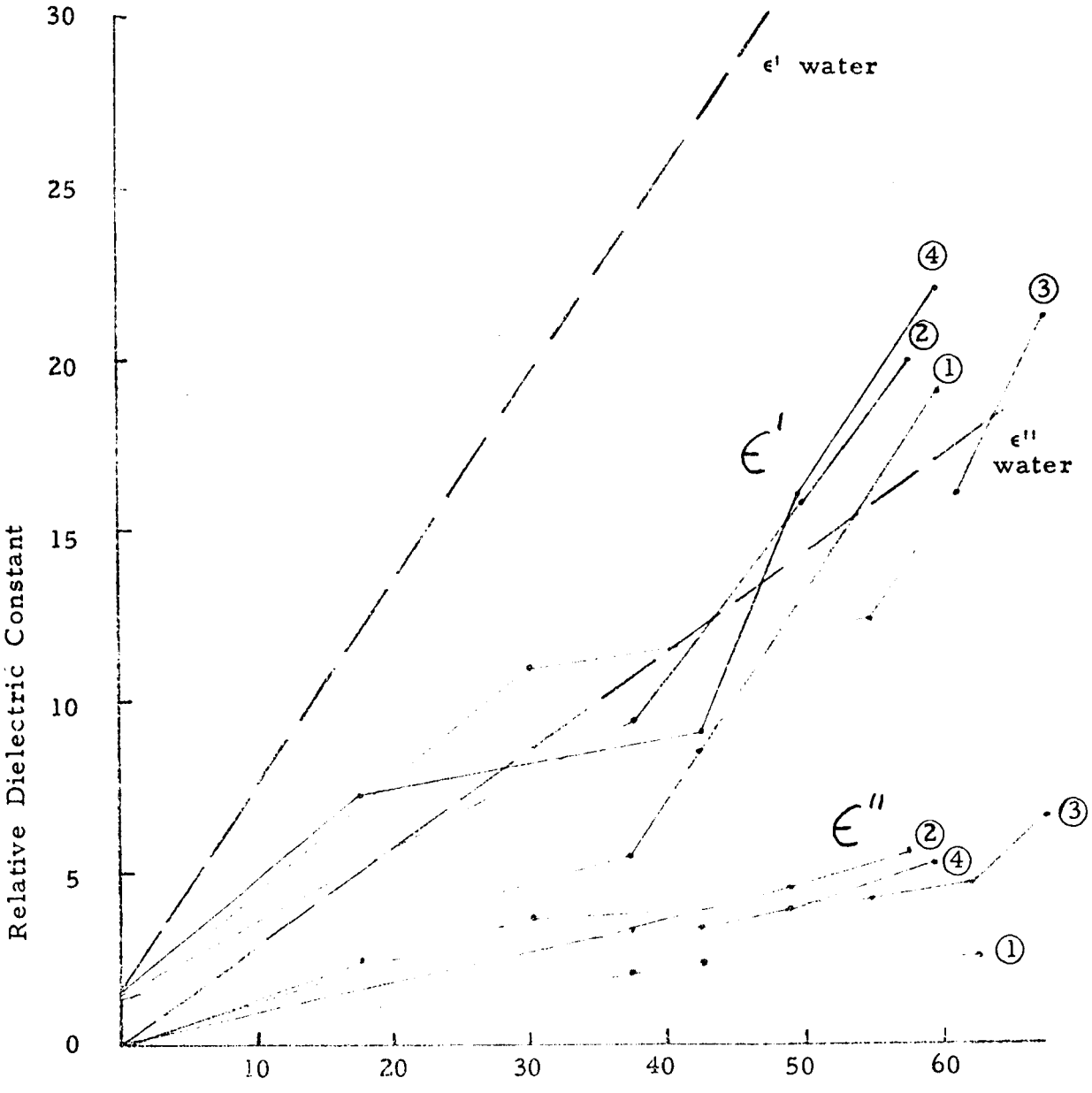

Fig. 16. The complex dielectric constant of corn leaf plotted as a function of moisture content. Curves 2, 3, and 4 represent samples taken from leaves of the same plant.

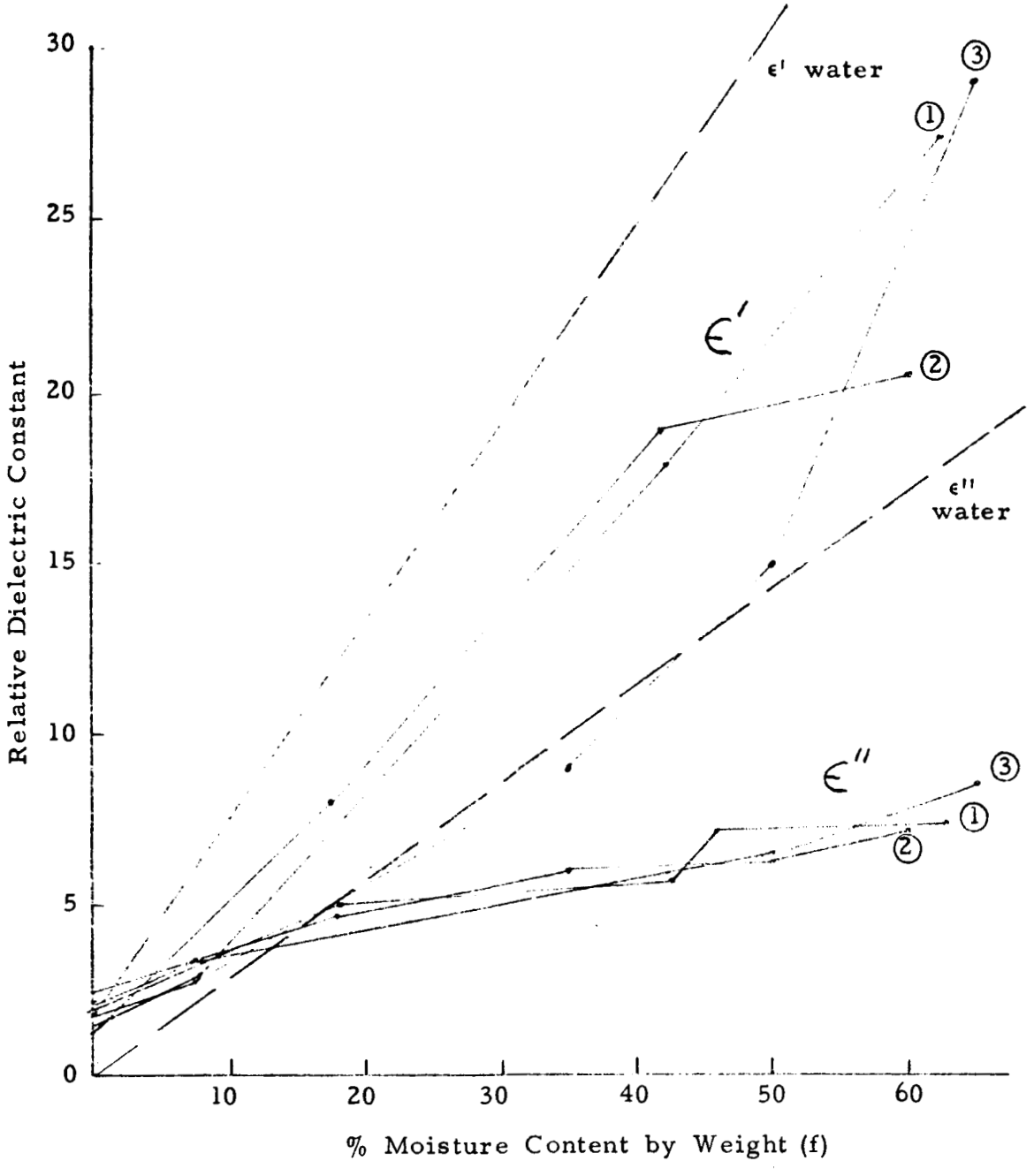

Fig. 17. The complex dielectric constant of a needle of taxus cuspidatus plotted as a function of moisture content.

It is instructive to compare these measured values with the known value for water at 8.5 GHz., 62 - j29.[14] If it were assumed that the water was contained in tubes parallel to the electric field, then ϵ for vegetation ought to be approximately that of an equivalent amount of water. This is clearly too large, (see dotted curves on Figs. 15 - 17). If, on the other hand, the tubes were perpendicular to the electric field the resultant dielectric constant should be closer to that of air. In this connection it would be of interest to observe the effect on the measurements if the leaf were placed with its vein structure perpendicular to the electric field, since it is known[1] that samples of wood, for example, exhibit different dielectric constants when the grain is oriented parallel or perpendicular to the electric field.

While it is clear from the figures that the dielectric constant of vegetation is not exactly proportional to that of some equivalent fraction of water, the dependence on moisture content can be approximately accounted for by a formula of the type below:

$$\epsilon' - j\epsilon'' = 1.5 + \left(\frac{\epsilon'_w}{2} - j\frac{\epsilon''_w}{3}\right) f \tag{68}$$

for the samples of corn, grass and taxus,
where:

$\epsilon' - j\epsilon''$ = the real and imaginary parts of the dielectric constant of vegetation

$\epsilon'_w - j\epsilon''_w$ = the real and imaginary parts of the dielectric constant of water

f = the fractional amount of moisture present in the vegetation.

It is hoped that this equation may prove useful in developing an understanding of the radar scattering from vegetation.

The dielectric constant of the blue spruce sample was somewhat lower than predicted by Eq. (68). The most probable explanation is that, as the sections of needle dried out, hollow cores developed within the sections. Thus the actual volume of matter was smaller than the external volume of the sample, (ℓtw), used in Eq. (65).

VII. SUMMARY AND CONCLUSIONS

A cavity perturbation method has been developed whereby the complex dielectric constant of vegetation can be measured. An analysis of cavity design and operation has been presented from which it is possible to build a cavity suitable for this purpose. Using this perturbation technique, measurements were made of the complex dielectric constants of several types of vegetation: grass blades, corn leaves and the needles of two evergreens.

Each of the samples exhibited a dielectric constant that was highly dependent on water content. The samples displayed a high dielectric constant (about half that of water) when they were freshly cut (about 65% moisture by weight) and then as the samples were allowed to dry out the dielectric constant diminished until only the dielectric constant of the fibrous plant structure could be measured.

This method is not limited to measuring vegetation. The permittivity or permeability of any sample for which the geometry is known may be measured by the same technique.

APPENDIX A

This section shows in detail the relation between the power level indicated by the power meter of line 4, Fig. 12, and the loaded Q of the circuit. Consider the diagram of Fig. 19. Off resonance, the incident wave of amplitude a, (a being complex) is reflected by the iris with amplitude -a. Near resonance, a portion of the wave will be transmitted through the iris and the reflected wave will be correspondingly reduced. The amplitude of the reflected wave at resonance may be represented by $-(a+a_o)$, and at the half power point by $-(a+a_1)$ where a_o and a_1 are amounts by which the reflected waves are reduced at resonance and half power respectively. If -b represents the reflected wave of line 2 the resultant waves in line 4 are:

$$\left(\frac{1}{\sqrt{2}}\right)\left[-(a+a_o)+b\right] \text{ and } \left(\frac{1}{\sqrt{2}}\right)\left[-(a+a_1)+b\right]$$

The power meter measures the quantity,

$$\left(\frac{1}{2}\right)\left|-(a+a_i)+b\right|^2 \qquad i = 0, 1$$

and since the circuit was previously adjusted off resonance so that a = b, the meter indication with respect to the power level at resonance is simply

$$\frac{|a_1|^2}{|a_o|^2}$$

Thus the meter will indicate a "half-power" point when $a_o = \sqrt{2}a_1$.

If a_1 and a_o are normalized with respect to a, the incident wave, the quantities $-1-a_1/a$ and $-1-a_o/a$ are equivalent to the reflection coefficient of the iris at half power and resonance respectively. That is,

$$\text{(A-1)} \qquad \Gamma_{res} = -1-\frac{a_o}{a} = \frac{1-\overline{g}}{1+\overline{g}}$$

$$\text{(A-2)} \qquad \Gamma_{\frac{1}{2}} = -1-\frac{a_1}{a} = \frac{1-\overline{g}-j\sqrt{\frac{\overline{C}}{\overline{L}}}\,\frac{2\,d\omega}{\omega_{res}}}{1+\overline{g}+j\sqrt{\frac{\overline{C}}{\overline{L}}}\,\frac{2d\omega}{\omega_{res}}}$$

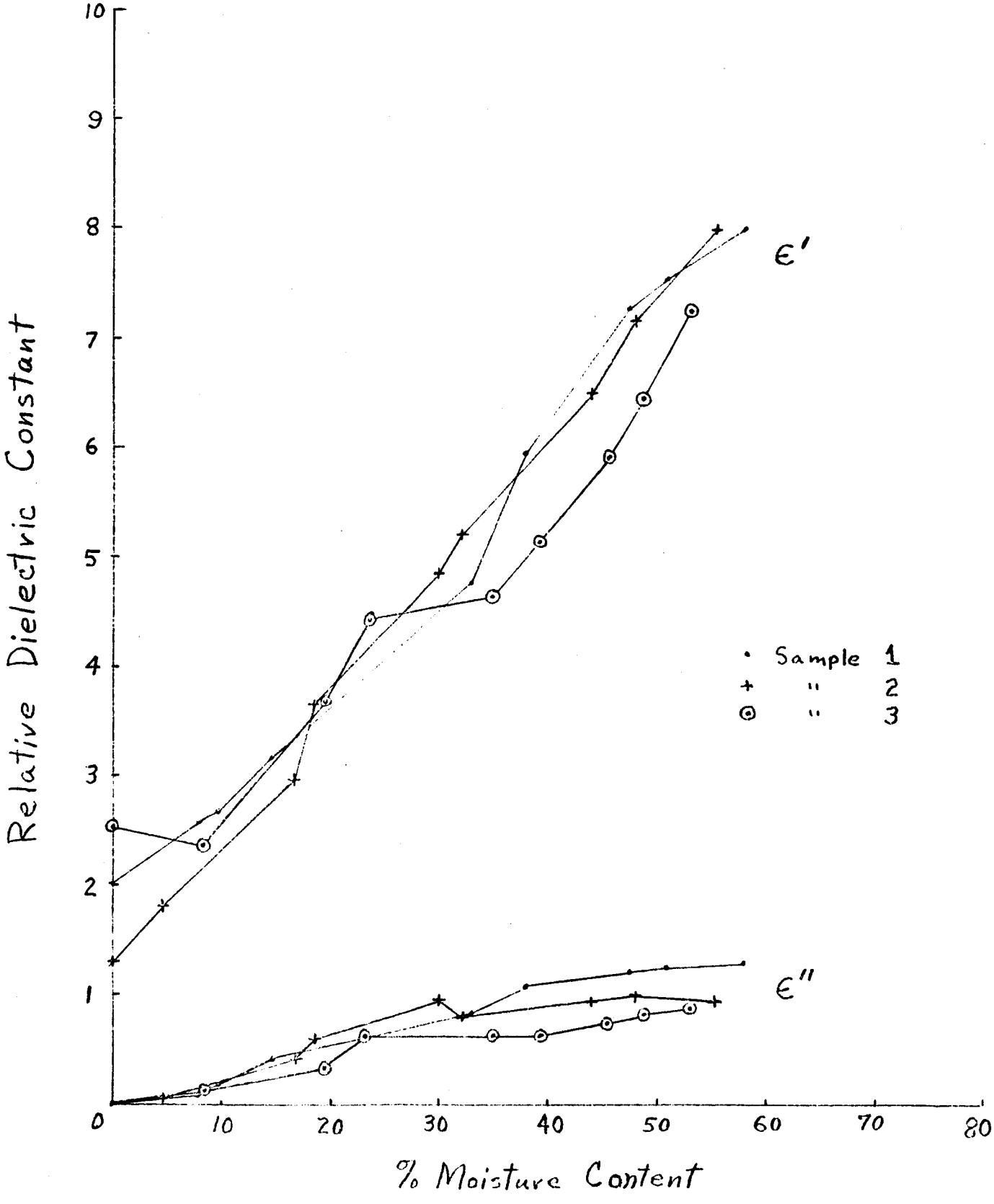

Fig. 18. Complex dielectric constant of blue spruce.

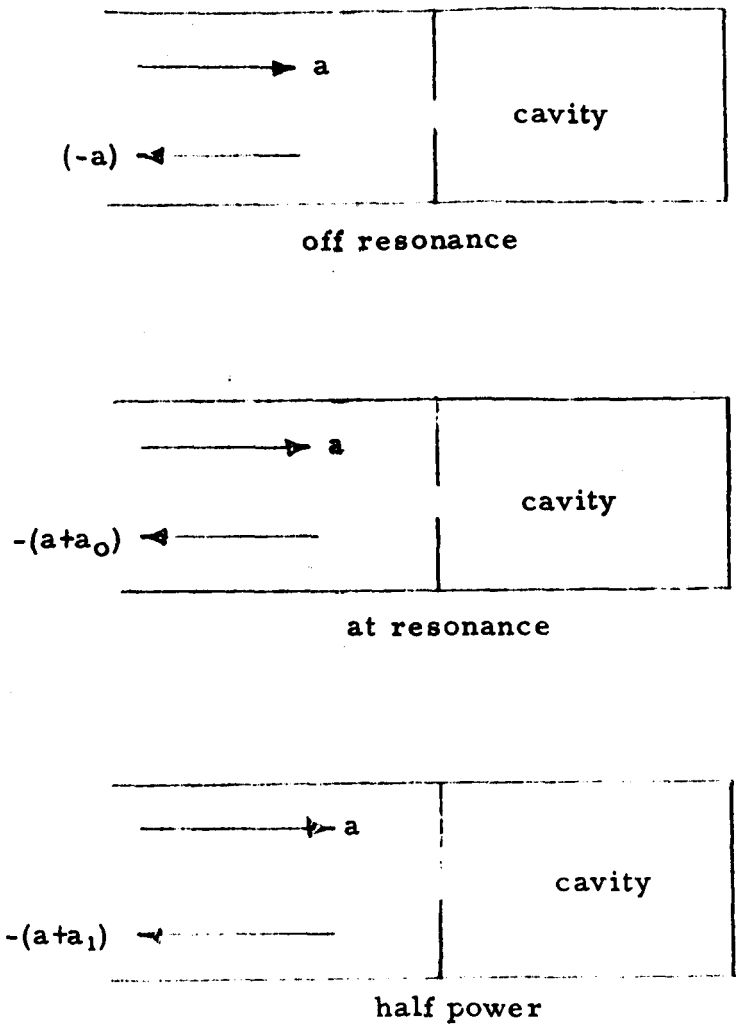

Fig. 19. The relation between the incident and reflected waves.

where $\bar{g}$, $\bar{L}$ and $\bar{C}$ are normalized elements of a shunt equivalent circuit for the cavity, see Fig. 20, and $d\omega = \omega - \omega_o$. Eqs. (A-1) and (A-2) reduce to

$$\text{(A-3)} \quad \frac{a_o}{a} = \frac{-2}{\bar{g}+1}$$

and

$$\text{(A-4)} \quad \frac{a_1}{a} = \frac{-2}{\bar{g}+1+j\sqrt{\frac{\bar{C}}{\bar{L}}}\,\frac{2d\omega}{\omega res}}$$

Thus,

$$\text{(A-5)} \quad \left|\frac{a_o}{a_1}\right|^2 = \frac{\left|\bar{g}+j\sqrt{\frac{\bar{C}}{\bar{L}}}\,\frac{2d\omega}{\omega_{res}}+1\right|^2}{(\bar{g}+1)^2}$$

or

$$\text{(A-6)} \quad \left|\frac{a_o}{a_1}\right|^2 = 1 + \frac{\frac{\bar{C}}{\bar{L}}\left(\frac{2d\omega}{\omega res}\right)^2}{(\bar{g}+1)^2}$$

Now since $Q_L = \sqrt{\frac{\bar{C}}{\bar{L}}}\,\frac{1}{1+\bar{g}}$, when $\left|\frac{a_o}{a_1}\right|^2 = 2$,

Eq. (A-6) yields

$$\text{(A-7)} \quad Q_L = \left(\frac{\omega res}{\Delta\omega}\right)$$

Here $\Delta\omega$ is twice $d\omega$ at the half power points, i.e. $\Delta\omega$ is the half power bandwidth observed on the power meter in line 4. Thus the half power bandwidth measured on a power meter at port 4 determines the loaded Q of the circuit.

To determine the unloaded Q, Q_u, which is the quantity required in the perturbation theory, the relation

$$\text{(A-8)} \quad \frac{1}{Q_L} = \frac{1}{Q_u} + \frac{1}{Q_E}$$

may be used. However, the required quantity is actually the difference between the reciprocals of the unloaded Q's of the perturbed and unperturbed cavity, see Eq. (66),

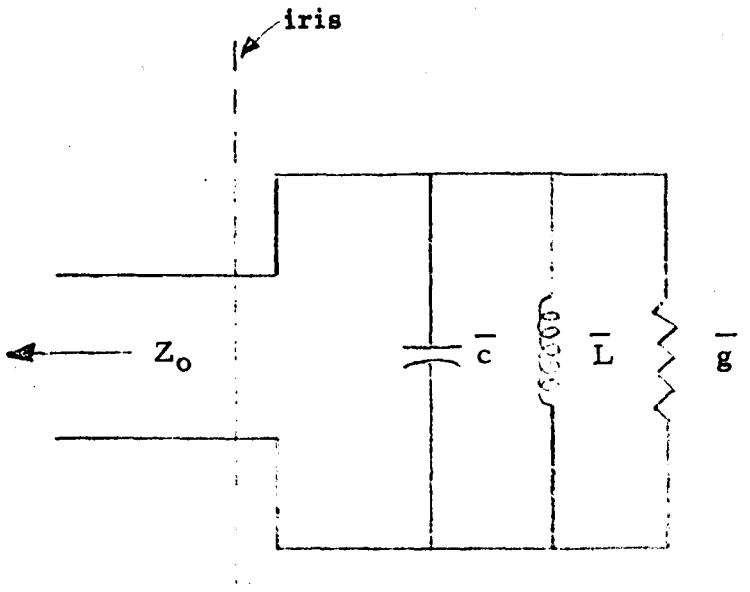

Fig. 20. Equivalent shunt circuit with the parameters $\overline{C}$, $\overline{L}$ and $\overline{g}$ normalized with respect to Z_o.

$$(A\text{-}9)\quad \underbrace{\left(\frac{1}{Q_L}-\frac{1}{Q_E}\right)}_{\text{perturbed}}-\underbrace{\left(\frac{1}{Q_{L_o}}-\frac{1}{Q_{E_o}}\right)}_{\text{unperturbed}}\approx 4\epsilon''\frac{\ell t\omega}{abc}$$

Since $Q_{E_o} \approx Q_E$ this equation reduces to

$$(A\text{-}10)\quad \frac{1}{Q_L}-\frac{1}{Q_{L_o}}\approx 4\epsilon''\frac{\ell t\omega}{abc}$$

Thus ϵ'' may be determined simply from the difference in the loaded Q's.

In practice it is desirable to have $Q_E >> Q_u$, in order to avoid the inaccuracies inherent in subtracting two nearly equal numbers in Eq. (A-9). The cavity used was designed to be considerably undercoupled. The measured normalized input admittance at resonance was found to be about 12. This is also the ratio of the external Q to the unloaded Q so that Q_E, which had a computed value of about 10,000, had only a small influence on the value of Q_L.

REFERENCE

1. Birks, J. B. and J. Hart. Progress in Dielectrics, Vol. 3, New York John Wiley and Sons, 1961

2. Harrington, Roger F. Time-Harmonic Electromagnetic Fields. New York, McGraw-Hill, 1961.

3. Ibid, p. 76

4. Ibid, p. 76

5. Collin, Robert E. Field Theory of Guided Waves. New York, McGraw-Hill, 1960.

6. Harrington, Roger F. op cit., p. 76

7. Altman, Jerome L. Microwave Circuits. Princeton, Van Nostrand, 1964.

8. Ibid, p. 54.

9. Ibid, p. 207.

10. Montgomery, C. G., R. H. Dicke, and E. M. Purcell. Principles of Microwave Circuits. New York, McGraw-Hill, 1948.

11. Harrington, Roger F. op cit., p. 322.

12. Altman, Jerome L. op cit., p. 412.

13. Cosgriff, R. L., W. H. Peake and R. C. Taylor. Terrain Scattering Properties for Sensor System Design. Columbus, Engineering Experiment Station Bulletin No. 181, The Ohio State University, 1960

14. Birks, J. B. op cit., p. 126.

15. Ammann, E. O. and R. J. Morris. "Tunable Dielectric-Loaded Microwave Cavities Capable of High Q and High Filling Factor," IEEE Transactions on Microwave Theory and Techniques, November 1963, pp. 528-542.

16. Marcuvitz, N. Waveguide Handbook. New York, McGraw-Hill, 1951.

17. Moreno, Theodore. Microwave Transmission Design Data. New York, Dover Publications, 1958.

18. Moore, Richard K. Traveling-Wave Engineering. New York, McGraw-Hill, 1960.

ACKNOWLEDGMENTS

The author wishes to thank Dr. William H. Peake for his helpful advice and guidance. Thanks are also owed to Terry L. Oliver for his assistance in making the measurements.